Protonic conductivity at the superionic phase transitions in the $M_3H(XO_4)_2$ crystal group

1999 J. Phys.: Condens. Matter 11 5099

(http://iopscience.iop.org/0953-8984/11/26/311)

J. Phys.: Condens. Matter **11** (1999) 5099–5110. Printed in the UK PII: S0953-8984(99)01578-7

Protonic conductivity at the superionic phase transitions in the $M_3H(XO_4)_2$ crystal group

Natalie I Pavlenko

Institute for Condensed Matter Physics of the National Academy of Sciences of Ukraine, 1 Svientsitsky Street, UA-290011 Lviv, Ukraine

E-mail: natalie@icmp.lviv.ua

Received 4 February 1999

Abstract. A microscopic model for the description of the proton subsystem dynamics in superionic crystals with hydrogen bonds is developed. Besides the inclusion of the proton-transport mechanism, the effect of the displacement of the nearest oxygens during hydrogen-bond formation is taken into account. The latter effect is the cause of the strong proton–phonon coupling that leads to the polaronic effect. Using the occupation number formalism, the virtual (in superionic phases) or ordered (in low-temperature phases) character of the hydrogen-bonded system is taken into account on the basis of the proton-ordering model. Protonic conductivity studies are carried out in the framework of the Kubo theory for the cases of superionic phases as well as low-temperature phases with different types of proton ordering (as an example the $M_3H(XO_4)_2$ class of crystals is considered). The temperature dependencies of the conductivity are analysed. The activation energies for the static conductivity are determined; for this case the influence of the internal field which appears as a result of the proton ordering is investigated.

1. Introduction

Hydrogen-bonded superionic crystals are well known for their proton orderings at low temperatures as well as for high protonic conductivity which increases significantly in the high-temperature superionic phases. In this case the conductivity phenomenon is connected with the dynamical disordering of the hydrogen-bond network, resulting in an increase of the number of possible positions for protons. It is generally accepted from the results of neutron scattering studies [1–3] that the proton transport proceeds in the framework of the two-stage Grotthuss mechanism. This process includes the transfer of the proton within the hydrogen bond (intrabond motion) and breaking of the hydrogen bond together with the reorientation of the ionic group involved in the hydrogen-bond formation (interbond transfer). Despite the detailed experimental investigation of the proton migration process, there still exist unresolved problems in the theoretical description of this phenomenon. This is due to the complexity of the problem of proton transport in the two- or three-dimensional hydrogen-bond network.

In this work the crystals which belong to the $M_3H(XO_4)_2$ (M = Rb, Cs, NH_4; X = Se, S) family are considered as the subjects for protonic conductivity investigations. In these compounds the conductivity is significantly higher in the conducting planes formed by the vertex O(2) oxygens connected by the virtual hydrogen bonds in superionic phases.

The crystals of this class are isomorphic, which explains the similarity of the phase sequences occurring in them. In most cases the superionic phase of trigonal symmetry transforms on cooling into a ferroelastic phase of monoclinic or triclinic symmetry with further

0953-8984/99/265099+12$19.50

ferroelectric ordering. The typical crystalline structure of the unit cell in the superionic phase with coordinates $\boldsymbol{R}_m = m_1\boldsymbol{a}_1 + m_2\boldsymbol{a}_2 + m_3\boldsymbol{a}_3$ in the rhombohedral coordinate system with the lattice vectors

$$\boldsymbol{a}_1 = \left(-\frac{\sqrt{3}}{2}a_0,\ \frac{1}{2}a_0,\ \frac{1}{3}c\right) \qquad \boldsymbol{a}_2 = \left(\frac{\sqrt{3}}{2}a_0,\ \frac{1}{2}a_0,\ \frac{1}{3}c\right) \qquad \boldsymbol{a}_3 = \left(0,\ -a_0,\ \frac{1}{3}c\right)$$

($a_0 = 3.5$ Å, $c = 22.9$ Å) is shown in figure 1. There are two XO_4 groups and three virtual hydrogen bonds, $f = 1, 2, 3$, adjacent to the upper group $XO_4^{(1)}$ in the elementary unit cell. Another three hydrogen bonds near the lower $XO_4^{(2)}$ group belong to the neighbouring unit cells with the vectors $\boldsymbol{R}_m - \boldsymbol{a}_f$.

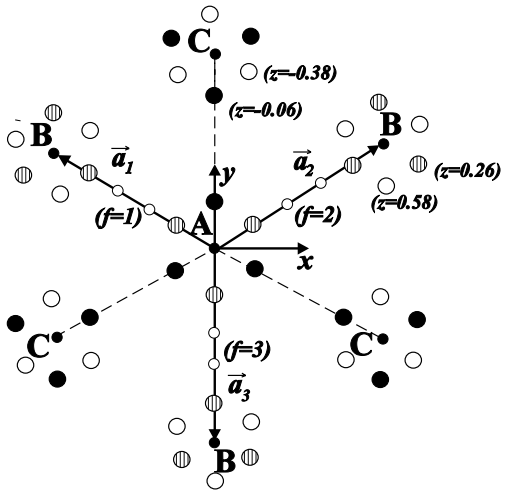

Figure 1. A projection of the rhombohedral primitive unit cell of $M_3H(XO_4)_2$ with lattice vectors $\boldsymbol{a}_1, \boldsymbol{a}_2, \boldsymbol{a}_3$ on the (001) plane in the hexagonal coordinate system in the superionic phase. The open, solid and hatched big circles correspond to the possible positions of O(2) oxygens with different values of z; A ($z = 0$), B ($z = 1/3$) and C ($z = -1/3$) denote the positions of X atoms in $XO_4^{(2)}$ groups. The small circles indicate the proton positions within the hydrogen bond.

In the low-temperature phase the frozen-in hydrogen bonds form well-defined sequences of dimers consisting of XO_4 tetrahedra connected by the $O(2)^{(1)}$–H–$O(2)^{(2)}$ hydrogen bridges. Two types of ordering with different characters of the dimer sequences can occur in this crystal class. In the first case (phase III for $(NH_4)_3H(SeO_4)_2$ (TAHSe), phase III for $Rb_3H(SeO_4)_2$ (TRHSe)) the doubling of the unit cell along one of the translation vectors $\boldsymbol{a}_f$ corresponds to the star $\{\boldsymbol{k}_4\} = \{\frac{1}{2}\boldsymbol{b}_1, \frac{1}{2}\boldsymbol{b}_2, \frac{1}{2}\boldsymbol{b}_3\}$ in Kovalev notation [4]. In particular, the alternating dimer sequences along the $\boldsymbol{a}_1$- and $\boldsymbol{a}_2$-directions are formed for the case where $\boldsymbol{k}_4 = \frac{1}{2}\boldsymbol{b}_3$.

Another type of ordering (phase IV in TAHSe, phase II in $(NH_4)_3H(SO_4)_2$) is distinguished by the parallel sequences of dimers which include hydrogen bridges of the same index f. However, the hydrogen bonds are shifted alternately by $\pm\delta$ ($\delta = 0.025b$ where b is the lattice parameter in phase IV) in the (x,y) plane. This corresponds to the ordering with the vector $\boldsymbol{k}_8 = \frac{1}{2}(\boldsymbol{b}_1 + \boldsymbol{b}_2 + \boldsymbol{b}_3)$.

The rearrangements of the hydrogen-bond network at the superionic phase transitions have been studied in the framework of the lattice-gas-type model given in [5] with the following

Hamiltonian:

$$H = \frac{1}{2}\sum_{\substack{mm'\\ ff'}} \Phi_{ff'}(mm')n_{mf}n_{m'f'} - \mu\sum_{mf} n_{mf} \tag{1}$$

where $n_{mf} = \{0, 1\}$ is the proton occupation number for position f in the primitive unit cell at $\boldsymbol{R}_m$; $\Phi_{ff'}(mm')$ is the energy of the proton interactions and μ denotes the chemical potential which determines the average proton concentration.

Investigations of the thermodynamic properties of the proton subsystem have been carried out in [5, 6] using the molecular-field approximation (MFA) as well as taking into account the short-range proton correlations. The influence of the XO_4 ionic group reorientations on the phase sequence has been also studied in [7]. It turned out that this effect is of primary importance for the description of the phase sequence occurring in TAHSe with two superionic (I, II) and two ferroelastic III and IV phases.

This work uses the results concerning the proton-ordering description for the evaluation of the protonic conductivity. It is shown that the distinction of the different types of hydrogen bonding (virtual in the superionic phases and ordered at low temperatures) leads to temperature dependencies of the protonic conductivity that are similar to the experimentally observed ones.

2. The polaronic effect and proton dynamics

It is well known from [8–10] that the creation of the hydrogen bond induces the deformation of the XO_4 groups involved in the bond formation. In particular, this process is accompanied by a shortening of the distance between the neighbouring vertex oxygens $O(2)^{(1)}$ and $O(2)^{(2)}$ that leads to the localization of the proton between these ions (the so-called polaronic effect) as well as to an increase of the activation energy for the bond breaking and hopping of the protonic polaron to another localized position in the lattice. To account for this fact one should determine the normal vibration modes of the vertex oxygen ions in the conducting planes.

The potential energy of the vertex oxygen subsystem in the harmonic approximation is given by

$$\phi = \phi_0 + \sum_{mm'}\sum_{kk'}\sum_{\alpha\beta=1,3} \phi_{\alpha\beta}(mk; m'k')u_\alpha(mk)u_\beta(m'k')$$

where $k = 1, 2$ is the sublattice number of the mth unit cell and the force constants

$$\phi_{\alpha\beta}(mk; m'k') = \left.\frac{\partial^2\phi}{\partial u_\alpha(mk)\,\partial u_\beta(m'k')}\right|_0 .$$

Taking into account the interaction between nearest neighbours in the (x, y) plane (the distances between the upper and lower sublattice oxygens O(2) in the cell are about 7.3 Å and exceed the separation between nearest oxygens in the (x, y) plane which amounts to 3.5 Å), the matrices $\phi(mk; m'k')$ can be represented in the following form:

$$\phi(m1; m + \boldsymbol{a}_1, 2) = \begin{pmatrix} \varphi_1 & \varphi_2 \\ \varphi_2 & \varphi_1 + (2/\sqrt{3})\varphi_2 \end{pmatrix}$$

$$\phi(m1; m + \boldsymbol{a}_2, 2) = \begin{pmatrix} \varphi_1 & -\varphi_2 \\ -\varphi_2 & \varphi_1 + (2/\sqrt{3})\varphi_2 \end{pmatrix}$$

$$\phi(m1; m + \boldsymbol{a}_3, 2) = \begin{pmatrix} \varphi_1 + \sqrt{3}\varphi_2 & 0 \\ 0 & \varphi_1 - \varphi_2/\sqrt{3} \end{pmatrix}$$

$$\phi(mk; mk) = \begin{pmatrix} \varphi_0 & 0 \\ 0 & \varphi_0 \end{pmatrix}.$$

Considering only displacements of the O(2) oxygens in the (x, y) plane, we have the following dynamical matrix:

$$D(\boldsymbol{k}) = \begin{bmatrix} D^{11} & D^{12} \\ D^{21} & D^{22} \end{bmatrix}$$

where $D^{12}(\boldsymbol{k})$ is

$$\begin{bmatrix} \varphi_1(\mathrm{e}^{\mathrm{i}\boldsymbol{k}\cdot\boldsymbol{a}_1} + \mathrm{e}^{\mathrm{i}\boldsymbol{k}\cdot\boldsymbol{a}_2}) + (\varphi_1 + \sqrt{3}\varphi_2)\mathrm{e}^{\mathrm{i}\boldsymbol{k}\cdot\boldsymbol{a}_3} & \varphi_2(\mathrm{e}^{\mathrm{i}\boldsymbol{k}\cdot\boldsymbol{a}_1} - \mathrm{e}^{\mathrm{i}\boldsymbol{k}\cdot\boldsymbol{a}_2}) \\ \varphi_2(\mathrm{e}^{\mathrm{i}\boldsymbol{k}\cdot\boldsymbol{a}_1} - \mathrm{e}^{\mathrm{i}\boldsymbol{k}\cdot\boldsymbol{a}_2}) & (\varphi_1 + 2\sqrt{3}\varphi_2)(\mathrm{e}^{\mathrm{i}\boldsymbol{k}\cdot\boldsymbol{a}_1} + \mathrm{e}^{\mathrm{i}\boldsymbol{k}\cdot\boldsymbol{a}_2}) + (\varphi_1 - \sqrt{3}\varphi_2)\mathrm{e}^{\mathrm{i}\boldsymbol{k}\cdot\boldsymbol{a}_3} \end{bmatrix}$$

and

$$D^{11}(\boldsymbol{k}) = D^{22}(\boldsymbol{k}) = \begin{bmatrix} \varphi_0 & 0 \\ 0 & \varphi_0 \end{bmatrix} \qquad D^{21}(\boldsymbol{k}) = D^{12}(-\boldsymbol{k}).$$

The problem of determination of the normal optical vibrational modes thus reduces to the evaluation of the eigenvalues (vibration frequencies) and polarization vectors of the matrix $D(\boldsymbol{k})$. In particular, for the case where $\boldsymbol{k} = 0$ we have

$$\omega_{1/3}(0) = \varphi_0 + (3\varphi_1 + \sqrt{3}\varphi_2) \qquad \omega_{2/4}(0) = \varphi_0 - (3\varphi_1 + \sqrt{3}\varphi_2) \tag{2}$$

$$\boldsymbol{u}_1 = \frac{1}{\sqrt{2}}\begin{pmatrix} 1 \\ 0 \\ 1 \\ 0 \end{pmatrix} \qquad \boldsymbol{u}_2 = \frac{1}{\sqrt{2}}\begin{pmatrix} 0 \\ -1 \\ 0 \\ 1 \end{pmatrix} \qquad \boldsymbol{u}_3 = \frac{1}{\sqrt{2}}\begin{pmatrix} 0 \\ 1 \\ 0 \\ 1 \end{pmatrix} \qquad \boldsymbol{u}_4 = \frac{1}{\sqrt{2}}\begin{pmatrix} -1 \\ 0 \\ 1 \\ 0 \end{pmatrix} \tag{3}$$

which points to the existence of two different types (in-phase and anti-phase) of oxygen vibration with different frequencies. A similar situation is observed for other specific positions of the Brillouin zone.

We should take into account the change of the proton potential on the hydrogen bond due to the anti-phase vibrations of the oxygen ions that leads to the shortening of the bond length. Thus the modes $j = 2$ and $j = 4$ are considered with the coordinates of the polarization vectors $\boldsymbol{u}_2$ and $\boldsymbol{u}_2$ approximated by their values at $\boldsymbol{k} = 0$. After that, the interaction of the protons with the oxygen vibrations can be represented in the second-quantization form

$$H_{pr-ph} = \sum_{mf}\sum_{kj} \tau_{mf}(\boldsymbol{k}j)(b_{\boldsymbol{k}j} + b^{+}_{-\boldsymbol{k}j})n_{mf} \tag{4}$$

where b^{+}_{kj}, b_{kj} are the phonon creation and annihilation operators of the jth optical branch for the vector $\boldsymbol{k}$. The coefficients $\tau_{mf}(\boldsymbol{k}j)$ are given by

$$\begin{aligned}
\tau_{m1}(\boldsymbol{k}j) &= -\sqrt{\frac{\hbar}{2NM\omega_j(\boldsymbol{k})}}\,\nabla V\left\{(u_{jx}(1) - (1/\sqrt{3})u_{jy}(1))\exp[\mathrm{i}\boldsymbol{k}\cdot\boldsymbol{R}_m]\right. \\
&\quad \left. - (u_{jx}(2) - (1/\sqrt{3})u_{jy}(2))\exp[\mathrm{i}\boldsymbol{k}\cdot(\boldsymbol{R}_m + \boldsymbol{a}_1)]\right\} \\
\tau_{m2}(\boldsymbol{k}j) &= \sqrt{\frac{\hbar}{2NM\omega_j(\boldsymbol{k})}}\,\nabla V\left\{(u_{jx}(1) + (1/\sqrt{3})u_{jy}(1))\exp[\mathrm{i}\boldsymbol{k}\cdot\boldsymbol{R}_m]\right. \\
&\quad \left. - (u_{jx}(2) + (1/\sqrt{3})u_{jy}(2))\exp[\mathrm{i}\boldsymbol{k}\cdot(\boldsymbol{R}_m + \boldsymbol{a}_2)]\right\} \\
\tau_{m3}(\boldsymbol{k}j) &= -\sqrt{\frac{\hbar}{2NM\omega_j(\boldsymbol{k})}}\,\nabla V\frac{2}{\sqrt{3}}\left\{u_{jy}(1)\exp[\mathrm{i}\boldsymbol{k}\cdot\boldsymbol{R}_m] - u_{jy}(2)\exp[\mathrm{i}\boldsymbol{k}\cdot(\boldsymbol{R}_m + \boldsymbol{a}_3)]\right\}
\end{aligned} \tag{5}$$

where $\nabla V = \partial V(\boldsymbol{r}_{mf} - \boldsymbol{R}^0_{m1})/\partial u_1(m, 1)$, where $\boldsymbol{r}_{mf}$ is the proton coordinate in the fth bond of the mth unit cell; $V(\boldsymbol{r}_{mf} - \boldsymbol{R}^0_{m1})$ is the interaction potential of the proton and the oxygen ion $\mathrm{O}(2)^{(1)}$ of the upper ionic group $\mathrm{XO}_4^{(1)}$; M is the oxygen-ion mass.

In addition, the vibration energy of the oxygen subsystem in the harmonic approximation is given by

$$H_{ph} = \sum_{\boldsymbol{k}j} \hbar\omega_j(\boldsymbol{k}) b^+_{\boldsymbol{k}j} b_{\boldsymbol{k}j}. \tag{6}$$

From the results of recent x-ray studies [11] it is known that the $O(2)^{(1)}$–$O(2)^{(2)}$ separation length can be reduced to 2.3–2.4 Å in the superionic phases which leads to near barrierless proton transfer in the hydrogen bond [12]. Thus the description of the proton mobility can be based on the assumption of a one-minimum proton potential on the bond. With this conjecture, the proton-transport process can be considered as the dynamical breaking and creation of the hydrogen bonds connected with the HXO_4^- ionic group rotations:

$$H_t = \Omega_R \sum_{\substack{m \\ f \neq f'}} \left\{ c^+_{mf} c_{mf'} + c^+_{m+\boldsymbol{a}_f - \boldsymbol{a}_{f'}, f} c_{mf'} \right\}. \tag{7}$$

Here c^+_{mf}, c_{mf} are the proton creation and annihilation operators. We represent the interbond proton transfer as the quantum pseudo-tunnelling between two states (two virtual hydrogen bonds) with corresponding transfer integral Ω_R.

We emphasize that a more comprehensive study of the protonic conductivity requires, besides considering the reorientational interbond proton transfer, taking into account additionally the intrabond proton tunnelling processes in the double-well proton potential on the hydrogen bond. By this means the two-stage Grotthuss transport mechanism could be described. The detailed analysis of the contributions of both components (reorientational and tunnelling) to the total protonic conductivity has revealed the dominant role of the first one in the static and low-frequency conductivity part. However, we find that the high-frequency conductivity has some peculiarities which arise due to the intrabond tunnelling; the results of these investigations will be presented elsewhere. Furthermore, in this work we will dwell in more detail on the analysis of the temperature behaviour of the protonic conductivity $\sigma(\omega, T)$ in the limit $\omega \to 0$ for the superionic and low-temperature ordered phases.

Applying the canonical Lang–Firsov transformation to the new equilibrium states of relaxed oxygens with the proton between them,

$$\tilde{H} = \mathrm{e}^{\mathrm{i}S} H \mathrm{e}^{-\mathrm{i}S}$$

where

$$S = \sum_{mf} n_{mf} v_{mf} \qquad v_{mf} = \mathrm{i} \sum_{\boldsymbol{k}j} \frac{\tau_{mf}(\boldsymbol{k}j)}{\hbar\omega_j(\boldsymbol{k})} (b_{\boldsymbol{k}j} - b^+_{-\boldsymbol{k}j}) \tag{8}$$

we have the following Hamiltonian:

$$\begin{aligned} \tilde{H} &= -\tilde{\mu} \sum_{mf} n_{mf} + \frac{1}{2} \sum_{\substack{mm' \\ ff'}} \tilde{\Phi}_{ff'}(mm') n_{mf} n_{m'f'} + \sum_{\boldsymbol{k}j} \hbar\omega_j(\boldsymbol{k}) b^+_{\boldsymbol{k}j} b_{\boldsymbol{k}j} + \tilde{H}_t \\ \tilde{H}_t &= \Omega_R \sum_{\substack{m \\ f \neq f'}} \left\{ c^+_{mf} c_{mf'} X_{ff'}(mm) + c^+_{m+\boldsymbol{a}_f - \boldsymbol{a}_{f'}, f} c_{mf'} X_{ff'}(m + \boldsymbol{a}_f - \boldsymbol{a}_{f'}, m) \right\} \end{aligned} \tag{9}$$

with the band-narrowing factor given by

$$X_{ff'}(mm') = \exp\left[- \sum_{\boldsymbol{k}j} \frac{\Delta\tau_{ff'}(mm'|\boldsymbol{k}j)}{\hbar\omega_j(\boldsymbol{k})} (b_{\boldsymbol{k}j} - b^+_{-\boldsymbol{k}j}) \right]$$

$$\Delta\tau_{ff'}(mm'|\boldsymbol{k}j) = \tau_{mf}(\boldsymbol{k}j) - \tau_{m'f'}(\boldsymbol{k}j).$$

Here,

$$\tilde{\mu} = \mu + \sum_{kj} \frac{|\tau_{mf}(kj)|^2}{\overline{h}\omega_j(k)} \qquad \tilde{\Phi}_{ff'}(mm') = \Phi_{ff'}(mm') - 2\sum_{kj} \frac{\tau_{mf}(kj)\tau_{m'f'}(-kj)}{\overline{h}\omega_j(k)}$$

are the proton chemical potential and the energy of interaction between protons, which are renormalized due to the lattice polarization and formation of the protonic polaron as a result.

The description of the proton ordering using Hamiltonian (9) without directly including the transfer term $\hat{H}_t$ has been performed in [5,7]. It is shown that the molecular-field approximation gives qualitatively correct results concerning the phase transition sequence in $M_3H(XO_4)_2$ crystals, although additional inclusion of the molecular-field fluctuations could provide a significant decrease of the transition temperatures. Therefore it is reasonable to first account for the fluctuations, because this makes possible a quantitative comparison between the results from the theoretical studies and experimental data.

3. Thermodynamical properties of the proton subsystem

As noted above, we will use the proton part of Hamiltonian (9) without including the transfer term for the description of the proton subsystem thermodynamics. For the estimation of the range of validity of such an approximation, let us consider the polaron band-narrowing factor

$$\langle X_{ff'}(mm')\rangle = \exp\left[-\frac{1}{2}\sum_{kj}\frac{|\Delta\tau_{ff'}(mm'|kj)|^2}{(\overline{h}\omega_j(k))^2}\,\mathrm{cotanh}\left(\frac{1}{2}\beta\overline{h}\omega_j(k)\right)\right]$$
$$= \exp\left[-\frac{5}{3}\frac{E_0}{\overline{h}\omega_0}\,\mathrm{cotanh}\left(\frac{1}{2}\beta\overline{h}\omega_0\right)\right].$$

Here the optical phonon branch frequencies $\omega_2(k) = \omega_4(k) = \omega_0$ are approximated by their values at the centre of the Brillouin zone and the polaron binding energy is

$$E_0 = \overline{h}^2(\nabla V)^2/2M(\overline{h}\omega_0)^2.$$

Furthermore, the strong-proton–phonon-coupling regime that leads to the formation of the small polarons is considered (we will see below that the strong polaron effect actually occurs in these systems). Setting $\tilde{E}_0 = E_0/|a| \sim 1$, $\overline{h}\omega_0/|a| \sim 0.6$ (where $a = (1/\sqrt{2})[\tilde{\Phi}_{11}(k = 0) - \tilde{\Phi}_{12}(k = 0)]$) we obtain that the polaron bandwidth δ is

$$\delta \sim \Omega_R\langle X_{ff'}(mm')\rangle \sim 0.1\Omega_R \tag{10}$$

for $\tau_0 \sim kT/|a| \sim 0.1$ and narrows exponentially with further temperature increase. Thus for $\tau > \tau_0$ the polaronic bands degenerate practically to localized states due to the difference in vibration phases of the neighbouring oxygen wave functions [13]. In this case the proton-transport process is solely phonon-activated hopping between localized positions in the lattice.

For the description of the different types of proton ordering existing in these superionic systems, we introduce the order parameters analogously to [5]. In particular, for the case of the orientation state characterized by the vector $k_4 = \frac{1}{2}b_3$ in phase III (TAHSe) and $k_7 = 0$ (phase IV when the H-bond shifts are neglected for simplicity), the two order parameters are given by

$$u = \frac{1}{\sqrt{2}}(\langle n_{1+}\rangle - \langle n_{2+}\rangle) \qquad v = \frac{1}{\sqrt{6}}(\langle n_{1+}\rangle + \langle n_{2+}\rangle - 2\langle n_{3+}\rangle) \tag{11}$$

(the labels $i = \{+, -\}$ correspond to even and odd indices m_3 of the mth unit cell respectively) with the thermodynamical averages $\langle n_{1-}\rangle = \langle n_{2+}\rangle$, $\langle n_{2-}\rangle = \langle n_{1+}\rangle$ and $\langle n_{3-}\rangle = \langle n_{3+}\rangle$. The

average proton concentration per unit cell

$$\bar{n} = \frac{1}{N}\sum_{mf}\langle n_{mf}\rangle = 1$$

for this crystal class.

To develop the expressions for the average proton occupancies $\langle n_{fi}\rangle$, we will use the high-density expansion method in the framework of the classification of the thermodynamical perturbation series in the corresponding powers of the $1/z$ parameter (where z is the number of neighbours interacting with a given proton). In this case the proton part of the Hamiltonian (9) can be rewritten in the form

$$\tilde{H}_{pr} = \tilde{H}_{MF} + (\tilde{H}_{pr} - \tilde{H}_{MF}) = \tilde{H}_{MF} + \tilde{H}'_{pr} \tag{12}$$

where the MFA Hamiltonian

$$\tilde{H}_{MF} = U_0 + \sum_{mf}(\gamma_f(m) - \mu)n_{mf} \qquad \text{where } U_0 = -\frac{1}{2}\sum_{\substack{mm'\\ff'}}\tilde{\Phi}_{ff'}(mm')\langle n_{mf}\rangle\langle n_{m'f'}\rangle$$

and the self-consistent internal fields

$$\gamma_f(m) = \gamma_{fi} = \sum_{m'f'}\tilde{\Phi}_{ff'}(mm')\langle n_{m'f'}\rangle$$

appear as a result of the long-range interactions between protons. The zero-order terms in the expansions for the averages $\langle\cdots\rangle = \langle\cdots\sigma(\beta)\rangle_0/\langle\sigma(\beta)\rangle_0$ (here $\sigma(\beta) = \exp(-\beta\tilde{H}'_{pr})$ and $\langle\cdots\rangle_0 = \mathrm{Sp}\cdots\mathrm{e}^{-\beta\tilde{H}_{MF}}/\mathrm{Sp}\,\mathrm{e}^{-\beta\tilde{H}_{MF}}$) with respect to the perturbation term $\tilde{H}'_{pr}$ lead to the molecular-field approximation and the fluctuation effects are to be introduced by the terms of higher order. In particular, choosing a certain infinite partial sum in the corresponding series, to account for the Gaussian fluctuations of the molecular field (GFA) [14], we obtain

$$\langle n_{fi}\rangle = \frac{1}{\sqrt{2\pi}}\int_{-\infty}^{\infty}\mathrm{d}\xi\ \mathrm{e}^{-\xi^2/2}\Lambda\bigl(y + \sqrt{2(x_2)^i_f}\xi\bigr) \tag{13}$$

where $\Lambda^{[l]}(y) = \partial^{l+1}Q(y)/\partial y^{l+1}$ are the lth-order semi-invariants, $Q(y) = \ln(1 + \exp(y))$ and $y = \beta(\mu - \gamma_{fi})$. Using the approach proposed in [15] which does not lead to unphysical results, the mean square Gaussian fluctuations for the sublattice (f, i) are given by

$$(x_2)^i_f = \frac{1}{N}\sum_{\boldsymbol{k}}\{\beta\bar{\Phi}(\boldsymbol{k})\bar{\Lambda}^{[1]}\beta\bar{\Phi}(\boldsymbol{k})\} \tag{14}$$

where the proton interaction Fourier transform matrix $\bar{\Phi}(\boldsymbol{k}) = \Re\{\Phi^{ii'}_{ff'}(\boldsymbol{k})\}$ and the second-order semi-invariants matrix renormalized by the Gaussian distribution

$$\bar{\Lambda}^{[1]} = \{\bar{\Lambda}^{[1]ii'}_{ff'}\}\delta_{ff'}(i - i') = \{\bar{\Lambda}^{[1]}_{fi}\} \qquad \bar{\Lambda}^{[1]}_{fi} = \frac{1}{\sqrt{2\pi}}\int_{-\infty}^{\infty}\mathrm{d}\xi\ \mathrm{e}^{-\xi^2/2}\Lambda^{[1]}\bigl(y + \sqrt{2(x_2)^i_f}\xi\bigr)$$

are introduced.

It is easy to verify that the stationarity conditions for the free energy F

$$\frac{\partial F}{\partial u} = \frac{\partial F}{\partial v} = \frac{\partial F}{\partial (x_2)^i_f} = 0 \tag{15}$$

are equivalent to equations (11) and (14) with the free energy of the following form:

$$F = -\frac{N}{2}(\gamma_0 + \sqrt{6}av^2 + \sqrt{2}bu^2) + \mu N\bar{n}$$
$$- \frac{\Theta}{4}\sum_{\boldsymbol{k}}\sum_{f}\sum_{i=\{+,-\}}(\beta\bar{\Phi}(\boldsymbol{k})\bar{\Lambda}^{[1]})^2_{fi} - \frac{N}{2}\Theta\sum_{fi}(\bar{Q}_{fi} - (x_2)^i_f\bar{\Lambda}^{[1]}_{fi}) \tag{16}$$

where $\Theta = kT$ and

$$\gamma_0 = \frac{\bar{n}}{3}\sum_{\substack{mm'\\ff'}}\tilde{\Phi}_{ff'}(mm') \qquad \bar{Q}_{fi} = \frac{1}{\sqrt{2\pi}}\int_{-\infty}^{\infty} \mathrm{d}\xi\ \mathrm{e}^{-\xi^2/2} Q\left(y + \sqrt{2(x_2)^i_f}\xi\right)$$

and $b = (1/\sqrt{6})(\tilde{\Phi}_{11}(\boldsymbol{k}_4) - \tilde{\Phi}_{12}(\boldsymbol{k}_4))$. Besides (15), from the condition $\partial F/\partial\mu = 0$ we obtain the equation for the proton chemical potential:

$$\bar{n} = \langle n_{1+}\rangle + \langle n_{2+}\rangle + \langle n_{3+}\rangle \tag{17}$$

which should be solved for the given proton concentration $\bar{n}$.

The self-consistent system of equations (11), (14) and (17) is computed numerically. The results of the investigations of stable regions corresponding to the different types of ordering are represented in the form of a phase diagram ($\tau, \tilde{b} = b/a$) in figure 2. The MFA phase diagram obtained in [5] ($(x_2)^i_f \to 0$) is shown in the inset for comparison. It is worthwhile noting that our approach yields a better agreement with the experiment than the previous results [5], significantly decreasing the critical temperatures. In particular, for $\tilde{b} = 1.688$, corresponding to TAHSe crystal [7], we have $T_c^{GFA} = 330$ K which agrees closely with the experimentally obtained value $T_c = 302$ K. Because of this, for the evaluation of the protonic conductivity we will take into account the temperature dependencies of the thermodynamical functions, average proton occupancies $\langle n_{fi}\rangle$ and proton chemical potential μ obtained in this section using the GFA.

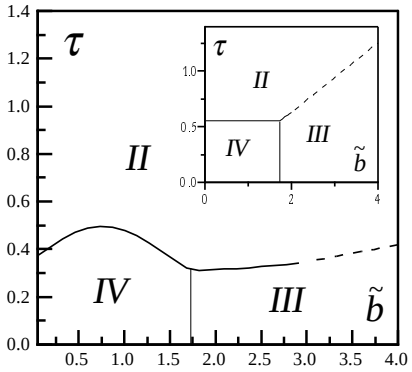

Figure 2. The $(\tau, \tilde{b})$ phase diagram obtained by including the Gaussian fluctuations of the molecular field (GFA); inset: the MFA results are shown for comparison. The full and broken curves indicate the first- and second-order phase transitions respectively.

4. Analysis of the protonic conductivity

The conductivity of the protons can be found in the framework of the Kubo linear response theory [16]:

$$\sigma(\omega, T) = \frac{1}{V}\int_0^{\infty} \mathrm{d}t\ \exp[\mathrm{i}(\omega + \mathrm{i}\varepsilon)t]\int_0^{\beta} \mathrm{d}\lambda\ \langle J(t - \mathrm{i}\bar{h}\lambda)J(0)\rangle \tag{18}$$

where V is the crystal volume and the proton current operator $J = (e/\mathrm{i}\bar{h})[\tilde{H}, x]$ ($x = \sum_{mf} n_{mf}\boldsymbol{r}_{mf}$ is the proton polarization operator). Furthermore, we will consider the polaronic transport which corresponds to phonon-activated hopping, because of the dominance of the contribution of this part to the total protonic conductivity at high temperatures [13]. The

polaronic current, which describes the hopping between the localized sites in the lattice, is given by

$$J_p = \frac{e\Omega_R}{\mathrm{i}\overline{h}} \sum_m \sum_{f\neq f'} \boldsymbol{R}_{ff'}[c^+_{mf}c_{mf'}\tilde{X}_{ff'}(mm) + c^+_{mf}c_{m+\boldsymbol{a}_f-\boldsymbol{a}_{f'},f'}\tilde{X}_{ff'}(m, m+\boldsymbol{a}_f-\boldsymbol{a}_{f'})]. \quad (19)$$

Here the vectors $\boldsymbol{R}_{ff'} = \boldsymbol{R}_{ff'}(mm) = \boldsymbol{r}_{mf} - \boldsymbol{r}_{mf'}$ connect the centres of the hydrogen bonds and the operators $\tilde{X}_{ff'}(mm') = X_{ff'}(mm') - \langle X_{ff'}(mm')\rangle$ characterize the phonon scattering processes which accompany the proton transfer. In this case the correlation function $\langle J_p(z)J_p(0)\rangle$ ($z = t - \mathrm{i}\overline{h}\lambda$) in (18) will be evaluated in the second-order perturbation theory applied to hopping term Ω_R. This allows us to decouple the following averages:

$$\langle c^+_{mf}(z)c_{m'f'}(z)\tilde{X}_{ff'}(mm')|_{t=z}c^+_{m_1f_1}c_{m'_1f'_1}\tilde{X}_{f_1f'_1}(m_1m'_1)\rangle$$
$$\rightarrow \langle c^+_{mf}(z)c_{m'f'}(z)c^+_{m_1f_1}c_{m'_1f'_1}\rangle\langle\tilde{X}_{ff'}(mm')|_{t=z}\tilde{X}_{f_1f'_1}(m_1m'_1)\rangle$$

into proton and phonon parts which can be evaluated separately. The proton correlators can be obtained by taking the proton part of the Hamiltonian (9) in the MFA:

$$\langle c^+_{mf}(z)c_{m'f'}(z)c^+_{m_1f_1}c_{m'_1f'_1}\rangle = \delta_{ff'_1}(m-m'_1)\delta_{f'f_1}(m'-m_1)\langle n_{mf}\rangle(1-\langle n_{m'f'}\rangle)$$
$$\times \exp\left[\frac{\mathrm{i}z}{2\overline{h}}[\gamma_f(m) - \gamma_{f'}(m') + \tilde{\Phi}_{ff'}(mm')(\langle n_{mf}\rangle - \langle n_{m'f'}\rangle)]\right]. \quad (20)$$

The processes that we are interested in are going on in the temperature range near the superionic phase transition. This allows us to assume that

$$\sum_{kj} \frac{|\Delta\tau_{ff'}(mm'|\boldsymbol{k}j)|^2}{(\overline{h}\omega_j(\boldsymbol{k}))^2 \sinh\frac{1}{2}\beta\overline{h}\omega_j(\boldsymbol{k})} \gg 1$$

which is valid at high temperatures and in the strong-proton–phonon-coupling regime. In this case, evaluation of the phonon correlation functions yields

$$\Psi_{ff'} = \langle\tilde{X}_{ff'}(mm')|_{t=z}\tilde{X}_{f'f}(m'm)\rangle$$
$$= \exp\left[-\sum_{kj}\frac{|\Delta\tau_{ff'}(mm'|\boldsymbol{k}j)|^2}{(\overline{h}\omega_j(\boldsymbol{k}))^2}\tanh\frac{1}{4}\beta\overline{h}\omega_j(\boldsymbol{k})\right]\exp\left[-\frac{(z+1/2\mathrm{i}\overline{h}\beta)^2}{4\tilde{\tau}^2}\right] \quad (21)$$

where the parameter $\tilde{\tau}$ which characterizes the average hopping time length between two localized positions is given by

$$\frac{1}{\tilde{\tau}^2} = 2\sum_{kj}\frac{|\Delta\tau_{ff'}(mm'|\boldsymbol{k}j)|^2}{\overline{h}^2\sinh\frac{1}{2}\beta\overline{h}\omega_j(\boldsymbol{k})} \qquad \tilde{\tau}^2 = \frac{3}{40}\beta\frac{\overline{h}^2}{E_0}. \quad (22)$$

We use the procedure proposed in [17] with the deformation of the integration contour in the complex plane for the integration of expressions (21) over t and λ. The resulting expression for the real part of the conductivity along the direction given by the vector $\boldsymbol{r}$ is the following:

$$\sigma(\omega)^r = \frac{e^2\Omega_R^2}{\overline{h}^2}\frac{2\sqrt{\pi}}{v_c}\frac{\sinh\beta\overline{h}\omega/2}{\overline{h}\omega/2}\exp\left[-\frac{5}{3}\beta E_0\right]\tilde{\tau}$$
$$\times \sum_{f\neq f'}(\boldsymbol{R}^r_{ff'})^2\langle n_{f+}\rangle(1-\langle n_{f'+}\rangle)\exp\left[\frac{1}{2}\beta\overline{h}\alpha_{ff'} - \tilde{\tau}^2(\omega+\alpha_{ff'})^2\right] \quad (23)$$

where v_c is the unit-cell volume, $\alpha_{ff'} = \Phi_0(1 - \langle n_{f+}\rangle + \langle n_{f'+}\rangle)/2\overline{h}$, $\Phi_0 = \tilde{\Phi}_{ff'}(m,m) = \tilde{\Phi}_{ff'}(m, m+\boldsymbol{a}_f-\boldsymbol{a}_{f'})$ is the interaction between the nearest neighbours and $\boldsymbol{R}^r_{ff'}$ is the projection of $\boldsymbol{R}_{ff'}$ on $\boldsymbol{r}$.

After consideration of (23), it becomes apparent that several different activation energies exist in the system:

$$E_a^{ff'} = \frac{5}{3}E_0 - \frac{1}{4}\Phi_0(1 - \langle n_{f+}\rangle + \langle n_{f'+}\rangle) + \frac{3}{160}\Phi_0^2(1 - \langle n_{f+}\rangle + \langle n_{f'+}\rangle)^2/E_0 \tag{24}$$

which correspond to the contributions of the different transfer processes (here we imply the polaron hopping between the different sublattices f) and appear in the expression for the conductivity with different weight factors which change with temperature. It should be noted that the total activation energy (24) consists of a polaronic part (the first term) and a part which appears as a result of the interproton interactions and proton orderings. Thus the temperature dependence of the different phonon-activated transfer processes is determined by the redistribution of the average proton occupancies of the three sublattices f. In particular, in the superionic phase where the hydrogen-bond network is disordered, there is only one activation energy: $E_a^0 = \frac{5}{3}E_0 - \frac{1}{4}\Phi_0 + \frac{3}{160}\Phi_0^2/E_0$.

In the low-temperature phase with the phase III (TAHSe) proton-ordering type ($\langle n_{1+}\rangle = 1$, $\langle n_{2+}\rangle = \langle n_{3+}\rangle = 0$ and $\langle n_{2-}\rangle = 1$, $\langle n_{1-}\rangle = \langle n_{3-}\rangle = 0$) in the saturation state, $E_a^{23} = \frac{5}{3}E_0 - \frac{1}{4}\Phi_0 + \frac{3}{160}\Phi_0^2/E_0$ with zero weight and $E_a^{12} = E_a^{13} = \frac{5}{3}E_0 > E_a^0$ if $E_0 > \frac{3}{40}\Phi_0$, which holds in the case of the strong polaronic effect. In the phase with the ordering of phase IV (TAHSe) type ($\langle n_{3i}\rangle = 1$, $\langle n_{1i}\rangle = \langle n_{2i}\rangle = 0$), the saturation activation energy $E_a^{31} = E_a^{32} = \frac{5}{3}E_0$. Therefore the activation energy in the ordered phases is always higher than that in the superionic phase, which agrees with the experimental observations [18, 19].

The temperature dependencies of the static conductivity evaluated using (23) along two different directions (210) and (010) in the (001) plane are shown in figures 3(a) and 4(a) for the different values of the polaron binding energy E_0 and for different types of phase transition. The corresponding average proton occupancies of sublattices f as functions of temperature are represented in figures 3(b) and 4(b). One can see that at $\tau = \tau_{si}$ (τ_{si} is the superionic phase transition temperature) the conductivity strongly increases, which corresponds to the kink in the logarithmic scale (see the insets). Furthermore, the increase of the energy E_0 leads to lower values of σ, which are evident due to the stronger localization of the proton in the hydrogen bond.

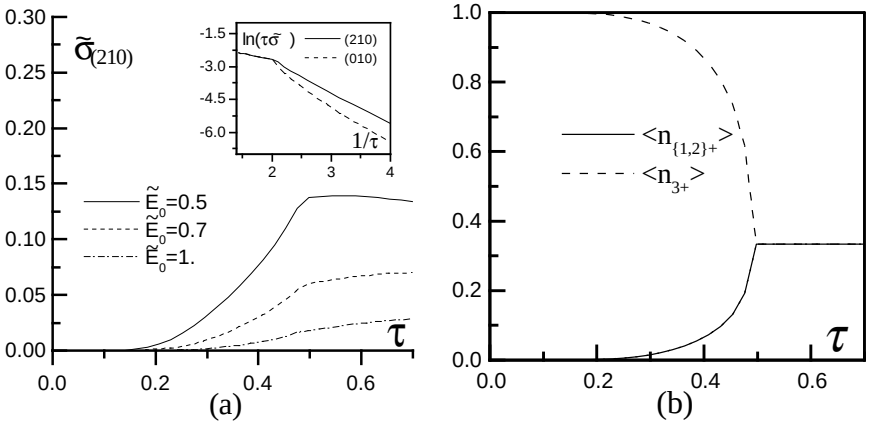

Figure 3. The temperature dependences of (a) the protonic conductivity $\tilde{\sigma} = \sigma/c_0$, where $c_0 = 2e^2a_0^2\Omega_R^2\sqrt{\pi}/\hbar v_c|a|^2$ for $\tilde{b} = 1$ (the first-order superionic phase transition to the ordered state with phase IV (TAHSe) proton-ordering type), $\Phi_0/|a| = 0.55$; inset: the case where $\tilde{E}_0 = 0.5$ on a logarithmic scale; and (b) the H-bond average proton occupancies obtained in the GFA.

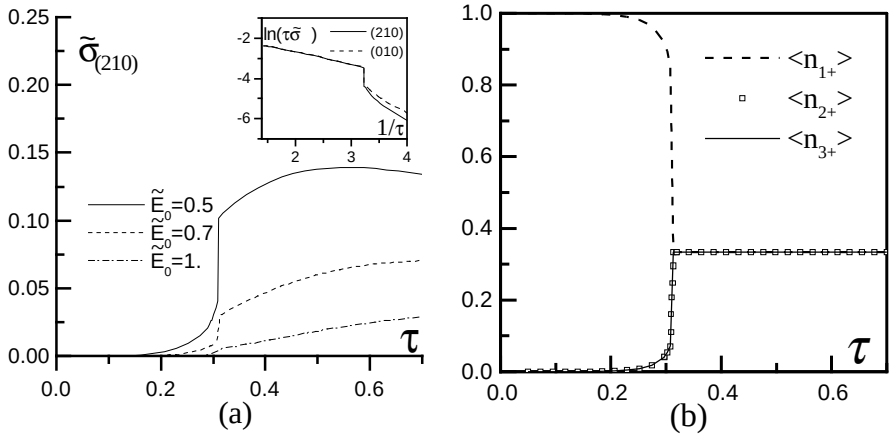

Figure 4. The temperature dependences of (a) the protonic conductivity $\tilde{\sigma}$ for $\tilde{b} = 1.73$ (the first-order superionic phase transition to the ordered state with phase III (TAHSe) proton-ordering type); inset: the case where $\tilde{E}_0 = 0.5$ on a logarithmic scale; and (b) the H-bond average proton occupancies obtained in the GFA.

Figure 5 shows the comparison of the theoretical conductivity obtained for TAHSe with the experimentally measured values [18]. The value of ∇V can be found from the dependence of the proton potential on the distance between the oxygen ions evaluated in [12], in this case $\nabla V = 2.4$ eV Å^{-1}. We can see that whereas in the superionic phase the two curves agree well, at low temperatures the measured conductivity is lower. The observed drop of σ at the phase transition is steeper than the calculated one. The values of the activation energy evaluated from (24) are the following: in the superionic phase $E_a^0 = 0.37$ eV and in the saturation states of the ordered phases $E_a = 0.4$ eV. Thus the theoretical activation energy in the superionic phase agrees well with the experimentally obtained value, ∼0.32 eV. However, in the ordered low-temperature phase the theoretical value is lower than the value ∼0.8 eV given in [18]. To obtain a better fit to the experimental data in the low-temperature region, it is necessary to take into account the additional short-range proton correlations which arise due to the polaronic effect and lead to the higher values of the activation energy in the ordered phases. The relation $E_0 > 2\Omega_R$ follows immediately from the values of the parameters in figure 5 and is valid for strong proton–phonon coupling (the small-polaron regime) [13].

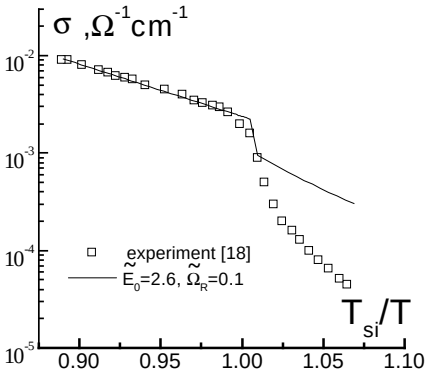

Figure 5. Comparison of the temperature dependencies of the protonic conductivity, measured for the crystal TAHSe and evaluated using (23) (in this case $\Omega_R = 70$ cm^{-1}, $\bar{h}\omega_0 = 455$ cm^{-1}).

5. Conclusions

In this work, the protonic conductivity in $M_3H(XO_4)_2$-type superionic crystals has been analysed in the framework of the proton-ordering model, additionally taking into account the reorientational proton-transfer processes. The one-minimum approximation has been considered for the proton potential within the hydrogen bond. The expression for the conductivity is obtained using the Kubo theory for the regime of strong coupling between protons and anti-phase vibrational modes of the oxygen ions involved in the H-bond formation, which leads to the shortening of this bond, localization of the proton and the strong polaronic effect. The following key points should be stressed. First, we note that taking into account the rearrangement of protons at the superionic phase transition provides the possibility of obtaining a temperature dependence of the protonic conductivity with the characteristic kink observed in experiments. Second, the activation energy evaluated for the superionic phase is lower than that for the ordered phases due to the proton localization on the hydrogen bond as well as the redistribution of the protons at the phase transition. The large polaron binding energy induces a significant decrease of the conductivity value. And finally, to obtain a better fit of our results with experiment for the low-temperature phases, the short-range correlations between protons should also be considered.

Acknowledgments

The author is greatly indebted to Professor I Stasyuk for useful and stimulating discussions. Partial financial support by the Ministry of Ukraine for Science and Technology (project No 2.4/174) is acknowledged.

References

[1] Belushkin A V, Carlile C J and Shuvalov L A 1995 *Ferroelectrics* **167** 21
[2] Lechner R E 1995 *Ferroelectrics* **167** 83
[3] Yamada Y 1995 *Ferroelectrics* **170** 23
[4] Kovalev O B 1986 *Irreducible and Inductive Representations and Corepresentations of Fedorov Groups* (Moscow: Nauka) (in Russian)
Kovalev O B 1965 *Irreducible Representations of the Space Groups* (New York: Gordon and Breach)
[5] Stasyuk I V, Pavlenko N and Hilczer B 1997 *Phase Transitions* **62** 135
[6] Stasyuk I V, Pavlenko N and Hilczer B 1998 *J. Korean Phys. Soc.* **32** S24
[7] Stasyuk I V and Pavlenko N 1998 *J. Phys.: Condens. Matter* **10** 7079
[8] Merinov B V, Bolotina N B, Baranov A I and Shuvalov L A 1980 *Crystallografiya* **33** 1387
[9] Merinov B V, Baranov A I and Shuvalov L A 1990 *Crystallografiya* **35** 355
[10] Merinov B V, Antipin M Yu, Baranov A I, Tregubchenko A M, Shuvalov L A and Struchko Yu T 1991 *Crystallografiya* **36** 872
[11] Pietraszko A, Hilczer B and Pawlowski A 1999 *Solid State Ion.* **119** 281
[12] Scheiner S 1992 *Proton Transfer in Hydrogen-Bonded Systems* ed T Bountis (New York: Plenum)
[13] Firsov Yu A (ed) 1975 *Polarons* (Moscow: Nauka) (in Russian)
[14] Izyumov Yu A, Kassan-Ogly F A and Skriabin Yu N 1974 *Field Methods in the Theory of Ferromagnets* (Moscow: Mir) (in Russian)
[15] Onyszkiewicz Z 1988 *Physica* B **151** 462
[16] Kubo R 1957 *J. Phys. Soc. Japan* **12** 570
[17] Reik H G and Heese D 1967 *J. Phys. Chem. Solids* **28** 581
[18] Pawlowski A, Pawlaczyk Cz and Hilczer B 1990 *Solid State Ion.* **44** 17
[19] Grigas J 1996 *Microwave Dielectrics Spectroscopy of Ferroelectrics and Related Materials* (New York: Gordon and Breach)